Article

Discovery Medicine 2025; 37(203): 2952–2965
https://doi.org/10.24976/Discov.Med.202537203.247

Mechanistic Insights Into Caveolin-1-Mediated Upregulation of Dynamin-2 in Podocyte Endocytosis During Diabetic Nephropathy

Xiangjing Wang[1], Yuanying Xia[1], Chengli Lou[1], Xiaoping Fan[1], Yijing Zhou[1,*], Kai Chen[2,*]

[1]Department of Nephrology, Jiaxing Hospital of Traditional Chinese Medicine, 314001 Jiaxing, Zhejiang, China
[2]Department of Pediatrics, Jiaxing Hospital of Traditional Chinese Medicine, 314001 Jiaxing, Zhejiang, China
*Correspondence: Jxzyy163@126.com (Yijing Zhou); jxzyychenkai@163.com (Kai Chen)
Submitted: 11 October 2025 Revised: 23 October 2025 Accepted: 10 November 2025 Published: 20 December 2025

Background: Diabetic kidney disease (DKD) remains a leading cause of end-stage renal disease globally, with podocyte injury recognized as a central contributor to proteinuria and disease progression. Caveolin-1 (Cav-1) has been implicated in the regulation of podocyte function, yet its precise role in DKD-related endocytosis and stress responses remains unclear. This study aimed to investigate the role of Cav-1 in podocyte injury, elucidate its molecular mechanisms in regulating endocytosis and stress signaling, and assess the potential contribution of Dynamin-2 in this process.

Methods: Cav-1 knockout mouse models and high-glucose-treated human podocytes (HPCs) were established. Western blotting, terminal deoxynucleotidyl transferase dUTP nick end labeling (TUNEL) staining, albumin endocytosis assays, and analyses of protein expression were performed to evaluate the effects of Cav-1 and Dynamin-2 on podocyte endocytic capacity and apoptosis. Expression of endocytosis-related molecules (clathrin heavy chain (CHC), Ras-related protein Rab 5 (Rab5), Rab7, EH-domain containing protein 2 (EHD2), Caveolae-associated protein 1 (CAVIN1)) and signaling pathway proteins (Src family kinases (SFKs), Ras homolog family member A (RhoA)) was also examined.

Results: Under high-glucose conditions, Cav-1 and endocytosis-related proteins (Dynamin-2, CHC, Rab5, Rab7) were significantly upregulated ($p < 0.05$), accompanied by enhanced podocyte endocytic activity ($p < 0.05$) and increased apoptosis ($p < 0.05$). Cav-1 deletion attenuated proteinuria and glomerular pathology in mice ($p < 0.05$), reduced the proportion of TUNEL-positive cells ($p < 0.05$), and suppressed the SFKs-RhoA signaling pathway as well as EHD2/CAVIN1 expression ($p < 0.05$).

Conclusion: Cav-1 serves as a central regulator of DKD-associated podocyte injury, promoting high-glucose-induced damage through cooperative interaction with Dynamin-2. Targeting Cav-1 and Dynamin-2 may provide a novel therapeutic approach to mitigate DKD progression and provide a theoretical basis for translating mechanistic insights into clinical applications.

Keywords: diabetic kidney disease; caveolin-1; dynamin-2; podocyte; endocytosis

Introduction

Diabetic kidney disease (DKD) is a microvascular complication of the kidney caused by chronic hyperglycemia [1]. Approximately 30%–40% of individuals with diabetes develop DKD, and about one-third of these cases progress to end-stage renal disease (ESRD), making DKD the leading cause of ESRD worldwide. This condition poses a major threat to human health and imposes a significant socioeconomic burden [2]. Clinically, DKD is characterized by persistent proteinuria and a progressive decline in glomerular filtration rate (GFR). Among these, elevated urinary protein is not only a hallmark of the disease but also a key risk factor contributing to disease progression and increased mortality [3,4]. Therefore, reducing proteinuria remains a central goal in delaying the progression of DKD. Although current therapeutic interventions, including renin-angiotensin-aldosterone system (RAAS) inhibitors, mineralocorticoid receptor antagonists (MRAs), sodium-glucose co-transporter 2 (SGLT2) inhibitors, and glucagon-like peptide-1 (GLP-1) receptor agonists, have shown partial efficacy in slowing DKD progression, they remain insufficient to prevent most patients from eventually developing ESRD [5–7].

In DKD pathogenesis, podocyte injury is recognized as a central event leading to proteinuria and disease progression [8]. Under hyperglycemic conditions, podocytes are exposed to multiple pathogenic stimuli, including oxidative stress, metabolic dysregulation, and inflammatory activation, which lead to structural and functional abnormalities such as foot process effacement, cytoskeletal disorganization, and enhanced apoptosis [9,10].

Endocytosis is essential for maintaining cellular homeostasis, and in podocytes, this process is vital for the development and maintenance of the glomerular filtration barrier. Dysregulation of podocyte endocytic pathways has

been associated with structural damage and dysfunction of the glomerular filtration barrier [11]. Therefore, elucidating the molecular mechanisms underlying podocyte injury and identifying novel therapeutic targets are crucial for optimizing DKD management.

Caveolin-1 (Cav-1) is a member of the structural protein family predominantly localized in caveolae, specialized plasma membrane invaginations present in various cell types [12]. As a key structural component of caveolae, Cav-1 not only provides mechanical stability but also regulates cholesterol metabolism, cell signaling, and endocytic processes [13–15]. In the kidney, Cav-1 is expressed in both podocytes and renal tubular epithelial cells, and its expression is regulated by high glucose, inflammatory mediators, and oxidative stress [16,17]. Previous studies have indicated that Cav-1 plays a critical role in glomerular diseases by regulating apoptosis, autophagy, and barrier integrity [18,19].

Recent research has also highlighted the critical role of Dynamin-2 (DNM2) in podocyte endocytosis. Dynamin-2 is a Guanosine Triphosphatase (GTPase) involved in receptor-mediated endocytosis and vesicle scission, and it interacts with the actin cytoskeleton to maintain the architecture of the podocyte foot processes [11]. A study has shown that inactivation of DNM1/DNM2 in podocytes leads to impaired endocytic activity, retention of endocytic pits, and abnormal deposition of actin/Actin-Related Protein 2 (Arp2)/3 complexes, leading to foot process injury and filtration barrier dysfunction [20]. Conversely, pharmacological or molecular enhancement of Dynamin activity promotes actin polymerization and alleviates podocyte injury and proteinuria phenotypes in mouse models of chronic kidney disease [21]. Additionally, mutations that affect Dynamin-2 membrane association or oligomerization have been shown to alter its regulation of stress fiber formation, thereby compromising podocyte stability at the cellular level [22].

Collectively, Cav-1 and Dynamin-2 play pivotal roles in linking endocytic mechanisms with cytoskeletal organization, thereby maintaining the structural and functional integrity of the glomerular filtration barrier. However, their interaction in regulating podocyte endocytosis and the modulation of this pathway under high-glucose conditions, which contribute to DKD progression, remains largely unclear. Therefore, the present study focused on the functional interplay between Cav-1 and Dynamin-2, aiming to elucidate their potential synergistic or antagonistic mechanisms in DKD. Understanding these interactions may provide valuable mechanistic insights into disease pathogenesis and identify novel therapeutic targets.

Materials and Methods

Animals

Cav-1 heterozygous (Cav-1$^{+/-}$) mice on a C57BL/6N background were generated by SAIYE Biotechnology Co., Ltd. (Guangzhou, China) using CRISPR/Cas9 gene-editing technology (Gene ID: 12389). Male Cav-1 knockout homozygotes (Cav-1$^{-/-}$) were obtained by mating male and female Cav-1$^{+/-}$ mice. Age-matched male wild-type C57BL/6N mice (8–10 weeks old, 22–24 g) served as the control group. Mice were maintained in a controlled environment at 22–26 °C with 40%–70% relative humidity and a 12-hour light/dark cycle in a quiet, noise-free facility. All housing equipment, feed, and bedding were routinely sterilized. The housing environment and materials complied with the standards of specific pathogen-free (SPF) animal facilities.

Grouping and Model Establishment

Male Cav-1 knockout (Cav-1$^{-/-}$) mice aged 6 weeks and weighing between 22 and 24 g were used in this study. Age-matched male C57BL/6N wild-type mice raised under identical environmental conditions served as controls. All animals were randomly assigned into four groups (n = 5 per group): Wild-type control (WT), Cav-1 global knockout (KO), wild-type diabetic kidney disease model (WT + Streptozotocin (STZ)), and Cav-1 knockout diabetic kidney disease model (KO + STZ).

Diabetes was induced in the experimental groups by intraperitoneal injection of streptozotocin (STZ; S0130, Sigma-Aldrich, MI, USA) at 50 mg/kg for five consecutive days following overnight fasting. STZ was freshly dissolved in 0.1 mol/L citrate buffer (pH 4.5) immediately before injection. Control mice received intraperitoneal injections of an equivalent volume of citrate buffer using the same schedule.

Body weight and blood glucose levels were monitored weekly. One week after STZ administration, blood glucose levels were measured using a portable glucometer (Accu-Chek Performa, Roche Diagnostics, Mannheim, Germany). Measurements were taken in the *ad libitum*-fed state, consistent with standard practice for validation of STZ-induced diabetes in mice. Mice with blood glucose levels exceeding 16.7 mmol/L were considered diabetic and included in further experiments, while those below this threshold were excluded. After 12 weeks of standard diet feeding, the experiment was concluded.

Twenty-four-hour urine samples were collected using metabolic cages, and urinary albumin-to-creatinine ratio (UACR) and total protein concentrations were determined using a Roche biochemical analyzer. Mice were anesthetized with isoflurane (51101, Sigma-Aldrich, MI, USA, induction at 3–4%, maintenance at 1–2% in oxygen) before tissue collection. Fresh renal tissues were excised, snap-frozen in liquid nitrogen for protein extraction, or fixed in

paraformaldehyde for histological analysis. At the end of the experiment, all animals were humanely euthanized by cervical dislocation under deep anesthesia induced by intraperitoneal injection of pentobarbital sodium (50 mg/kg), following the international guidelines for the care and use of laboratory animals.

Histological Staining Analysis

Kidney tissues were fixed in 4% paraformaldehyde (158127, Sigma-Aldrich, MI, USA) for 24 h, dehydrated through graded ethanol, cleared in xylene, and embedded in paraffin. Paraffin blocks were sectioned at 4 μm thickness, deparaffinized, and rehydrated through a descending alcohol series. For hematoxylin and eosin (H&E) staining (C0105S, Beyotime, China), sections were stained with hematoxylin for 5 min, rinsed in tap water, differentiated in 1% acid alcohol, blued in 0.2% ammonia water, and counterstained with eosin for 1–2 min. For Masson's trichrome staining (HT15, Sigma-Aldrich, MI, USA), sections were mordanted in Bouin's solution at 56 °C for 1 h, followed by sequential staining with Weigert's iron hematoxylin (10 min), Biebrich scarlet-acid fuchsin (10 min), phosphomolybdic–phosphotungstic acid (10 min), and aniline blue (5 min).

For periodic acid-Schiff (PAS) staining (395B, Sigma-Aldrich, MI, USA), sections were oxidized in 1% periodic acid solution for 10 min, stained with Schiff reagent for 15 min, and counterstained with hematoxylin for 2 min. All sections were then dehydrated, cleared, and mounted with neutral balsam. Histopathological changes, including glomerular morphology, inflammation, fibrosis, and glycogen deposition, were examined under a light microscope (Leica, Germany).

Cell Culture and Stimulation

Human podocytes (HPCs) were obtained from AcceGen (ABC-H0004Y, NJ, USA). Cell identity was authenticated by short tandem repeat (STR) profiling, as provided by the supplier, confirming human origin and the absence of cross-contamination. Mycoplasma contamination was routinely tested using polymerase chain reaction (PCR)-based assays, and all results were negative.

Cells were cultured in low-glucose Dulbecco's modified Eagle medium (DMEM; 5.5 mmol/L glucose, Gibco, USA) supplemented with 10% fetal bovine serum (FBS) and 1% penicillin–streptomycin at 37 °C in a humidified incubator with 5% CO_2. The normal-glucose (NG) condition was defined as a glucose level of 5.5 mmol/L. The high-glucose (HG) condition was established by supplementing D-glucose to a final concentration of 20 mmol/L. An osmotic control (OC) medium was prepared by adding mannitol to the NG medium to match the osmolarity of the HG medium.

Cav-1 Knockdown Experiment

Cav-1 expression was silenced using short hairpin RNA (shRNA) lentiviral vectors (GeneChem, Shanghai, China). Cells were divided into three groups: non-transfected control (NC), negative control shRNA (sh-NC), and Cav-1 knockdown (sh-Cav-1). The specific shRNA target sequence for Cav-1 was 5′-GACGTGGTCAAGATTGACTTT-3′ [23]. The negative control shRNA sequence (5′-TTCTCCGAACGTGTCACGT-3′) was provided by GeneChem (Shanghai, China).

Transfections were performed using Lipofectamine™ 2000 reagent (11668019, Thermo Fisher Scientific, MA, USA) following the manufacturer's instructions. Cells were harvested 48 h post-transfection. The knockdown efficiency was confirmed at both mRNA and protein levels using quantitative real-time PCR (qRT-PCR) and Western blot analysis.

Dynamin-2 Overexpression Experiment

The full-length cDNA of mouse Dynamin-2 (NM_010065) was cloned into the pLenti6.3_MCS_IRES2-EGFP lentiviral vector containing an N-terminal FLAG tag. Cells were assigned to three groups: non-transfected control (NC), empty vector-transfected control (overexpression control, OE-NC), and Dynamin-2 overexpression (OE-Dynamin-2). The construct was sequence-verified before transfection. Transfections were performed using Lipofectamine™ 2000 reagent under identical conditions, and cells were collected 48 h post-transfection. Overexpression efficiency was confirmed by qRT-PCR and Western blot analyses.

Endocytic Capacity Assay

Albumin uptake was used to evaluate receptor-mediated endocytosis in podocytes. Cells were incubated in serum-free medium (21041025, Thermo Fisher Scientific, MA, USA) containing fatty acid-free bovine serum albumin at a final concentration of 5 mg/mL. Cells were serum-starved for 30–60 min at 37 °C and subsequently stimulated with albumin for 2 h under starvation conditions. After incubation, cells were washed three times with PBS to remove residual medium. Cytoplasmic proteins were extracted using a cytoplasmic protein extraction kit (P0033, Beyotime, Shanghai, China), and intracellular albumin levels were determined by Western blot analysis.

Apoptosis Assay

Cell apoptosis was evaluated using the terminal deoxynucleotidyl transferase dUTP nick end labeling (TUNEL) staining kit (11684795910, Roche Diagnostics, IN, USA) following the manufacturer's instructions, and fluorescent signals were visualized under a fluorescence microscope.

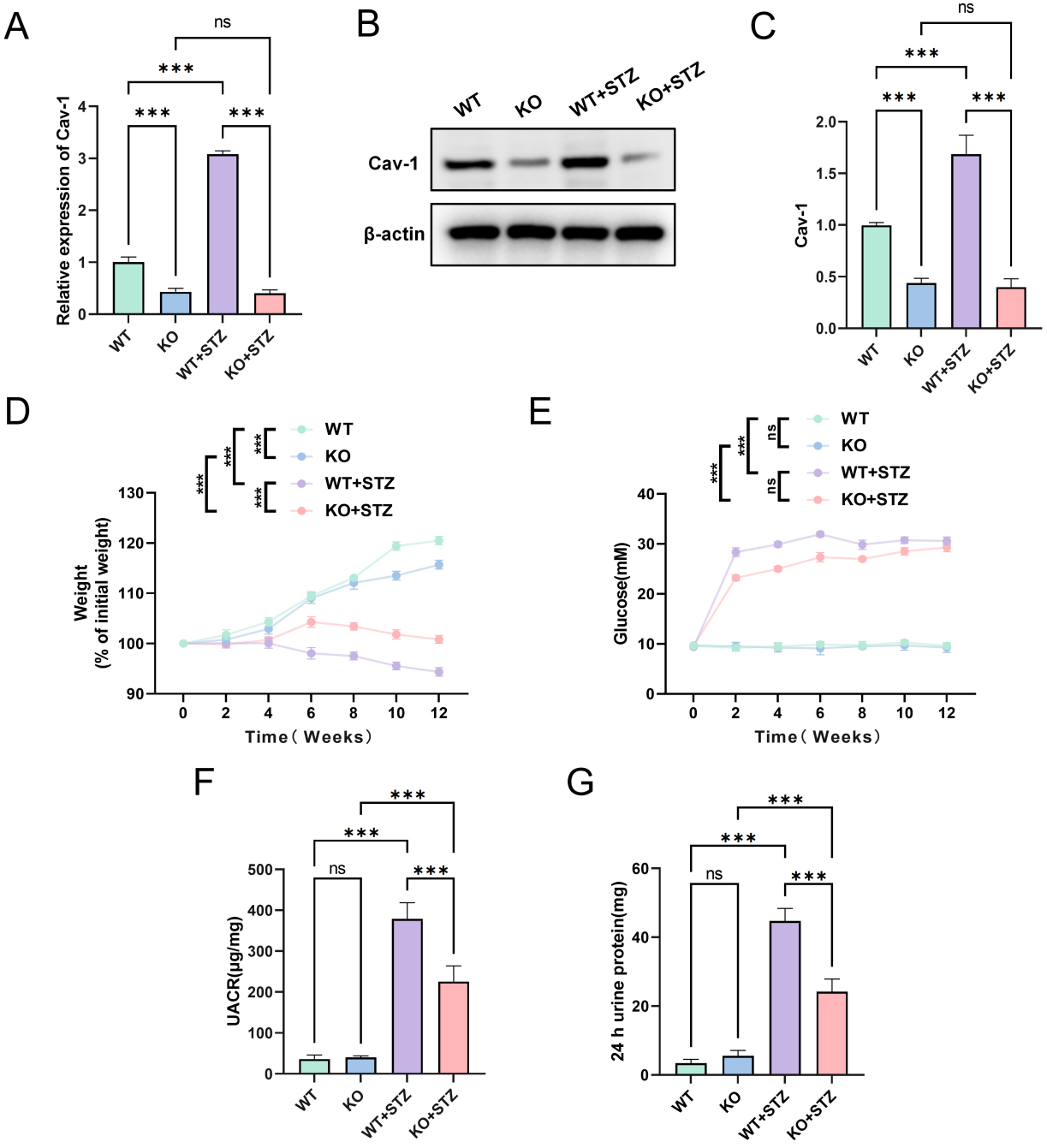

Fig. 1. Effects of Cav-1 knockout on renal function in diabetic kidney disease model mice. (A) Verification of Cav-1 expression by qRT-PCR, showing a significant reduction but not complete loss of Cav-1 expression in Cav-1-deficient mice. (B,C) Western blot analysis confirming markedly decreased Cav-1 protein levels, indicating successful partial knockout. (D) Changes in body weight of mice. Statistical significance represents comparisons among groups at the 12th week. (E) Alterations in blood glucose levels of mice (measured in the *ad libitum* feeding conditions). Statistical significance represents comparisons among groups at the 12th week. (F) Urinary albumin-to-creatinine ratio (UACR). (G) Twenty-four-hour urinary protein excretion. Statistical significance for body weight (D) and blood glucose (E) was determined by comparing the results with those of the WT group. n = 5; $^{***}p < 0.001$, $^{ns}p > 0.05$. Cav-1, Caveolin-1; qRT-PCR, quantitative real-time PCR.

RNA Extraction and qRT-PCR

Total RNA was extracted from kidney tissues using TRIzol reagent (15596018, Thermo Fisher Scientific, MA, USA) and treated with DNase I (11284932001, Sigma-Aldrich, MI, USA) to eliminate genomic DNA contamination. One microgram of total RNA was reverse-transcribed

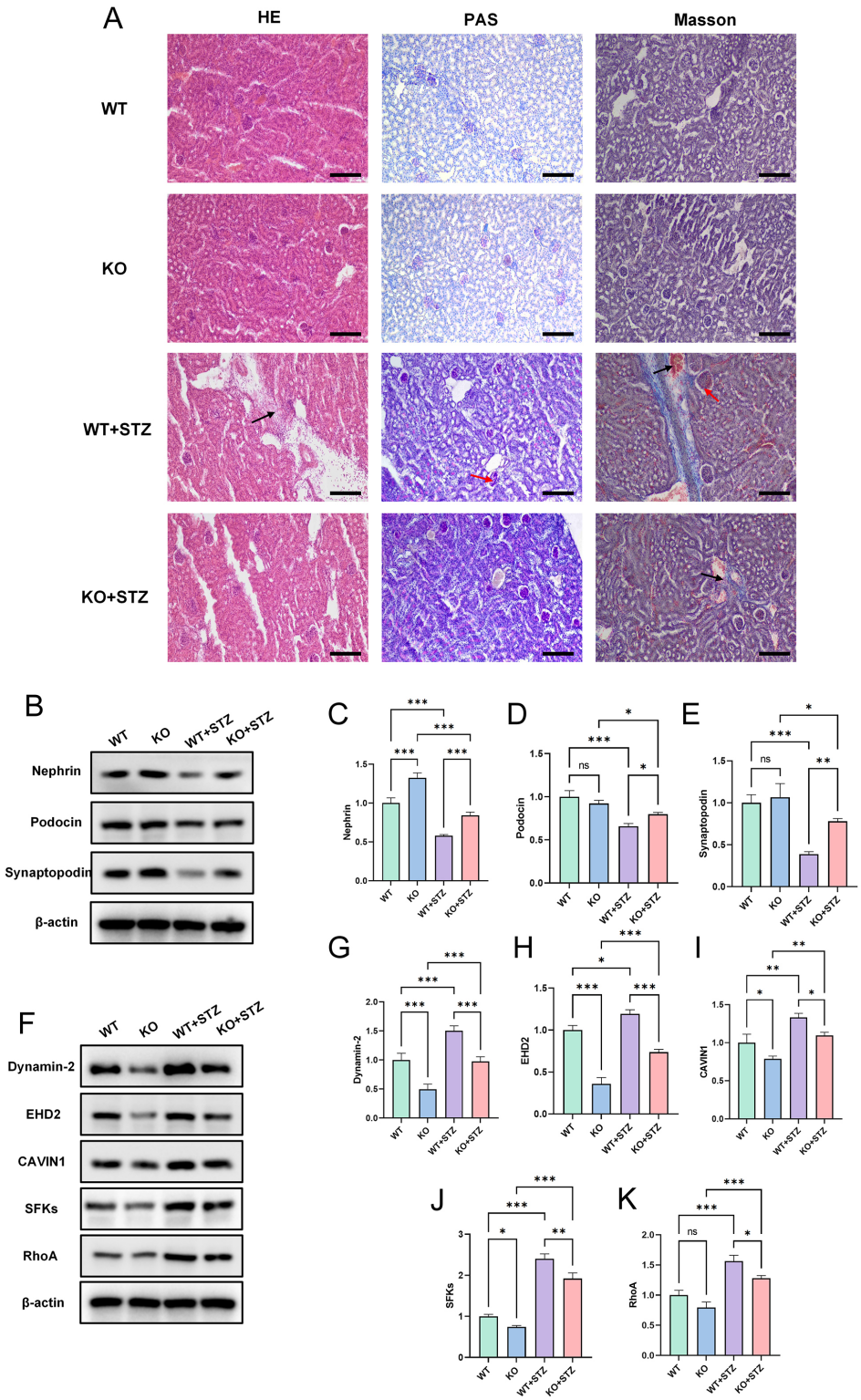

Fig. 2. Effects of Cav-1 knockout on renal tissue injury and podocyte alterations in mice. (A) Representative histopathological changes in mouse kidney tissues. Scale bar: 100 μm. Black arrows indicate inflammatory cell infiltration, and red arrows indicate glomerular hypertrophy and sclerosis. (B–E) Western blot analysis of Nephrin, Podocin, and Synaptopodin protein expression levels. (F–K) Western blot analysis of Dynamin-2, EHD2, CAVIN1, SFKs, and RhoA protein expression. n = 5; ***$p < 0.001$, **$p < 0.01$, *$p < 0.05$, $^{ns}p > 0.05$. EHD2, EH-domain containing protein 2; SFKs, Src family kinases; RhoA, Ras homolog family member A.

Table 1. Primer sequences used for qRT-PCR.

Gene	Forward Sequence (5′–3′)	Reverse Sequence (5′–3′)	Species
Cav-1	CAGGACGAGGAGGAGATGGA	GGTGACTTCTGCTGGAAGGT	*Mus musculus*
Dynamin-2	AAGGAGGAGATGCCAGAGGA	CTTGGTGGTGATGGTGGTGA	*Mus musculus*
β-actin	AGAGGGAAATCGTGCGTGAC	CAATAGTGATGACCTGGCCGT	*Mus musculus*
Cav-1	CCAAGGAGATCGACCTGGTCAA	GCCGTCAAAACTGTGTGTCCCT	*Homo sapiens*
Dynamin-2	AAAAGCAGCCCTGTGAGGCATG	GTGATCTCCAGGCTGATGAGCT	*Homo sapiens*
β-actin	CACCATTGGCAATGAGCGGTTC	AGGTCTTTGCGGATGTCCACGT	*Homo sapiens*

Cav-1, Caveolin-1; qRT-PCR, quantitative real-time PCR.

Table 2. Primary antibodies used for Western blot analysis.

Antibody	Supplier	Catalog number	Dilution ratio
Albumin	Abcam, Cambridge, UK	ab207327	1:2000
Cav-1	Cell Signaling Technology (CST), MA, USA	3267	1:1000
Nephrin	Abcam, Cambridge, UK	ab58968	1:1000
Podocin	Abcam, Cambridge, UK	ab181143	1:1000
Synaptopodin	Abcam, Cambridge, UK	ab224491	1:1000
EHD2	Abcam, Cambridge, UK	ab154784	1:1000
CAVIN1	Proteintech, IL, USA	11411-2-AP	1:1000
SFKs	CST, MA, USA	9320	1:1000
RhoA	Abcam, Cambridge, UK	ab187027	1:1000
CHC	Abcam, Cambridge, UK	ab21679	1:2000
Dynamin-2	Abcam, Cambridge, UK	ab3457	1:1000
Rab5	CST, MA, USA	3547	1:1000
Rab7	CST, MA, USA	9367	1:1000
β-actin	Abcam, Cambridge, UK	ab8226	1:1000

EHD2, EH-domain containing protein 2; SFKs, Src family kinases; CHC, clathrin heavy chain; Rab5, Ras-related protein Rab 5; CAVIN1, Caveolae-associated protein 1; RhoA, Ras homolog family member A.

into cDNA using the High-Capacity cDNA Reverse Transcription Kit (4368814, Thermo Fisher Scientific, Waltham, MA, USA). Quantitative real-time PCR was performed using a qRT-PCR kit (11732088, Thermo Fisher Scientific, Waltham, MA, USA). Relative mRNA expression levels of target genes were normalized to β-actin using the $2^{-\Delta\Delta Ct}$ method. Primer sequences are provided in Table 1.

Western Blot Analysis

Total protein was extracted from mouse kidney tissue samples and HPC cells were lysed in Radioimmunoprecipitation Assay (RIPA) buffer. Protein concentrations were determined using a Bicinchoninic Acid (BCA) protein assay kit (P0012, Beyotime, Shanghai, China). Equal amounts of protein (20 µg) were separated by polyacrylamide gel electrophoresis (PAGE) and transferred onto Polyvinylidene Fluoride (PVDF) membranes. The membranes were blocked with 5% non-fat milk for 1 h at room temperature, followed by overnight incubation at 4 °C with primary antibodies (Table 2). After incubation with primary antibodies, membranes were washed three times with Tris-Buffered Saline with Tween 20 (TBST) and subsequently incubated with appropriate Horseradish Peroxidase (HRP)-conjugated secondary antibodies for 1 h at room temperature. The secondary antibodies used included goat anti-rabbit Immunoglobulin G (IgG)-HRP (ab6721, Abcam, Cambridge, UK, 1:2000) and goat anti-mouse IgG-HRP (ab205719, Abcam, Cambridge, UK, 1:2000). Protein bands were visualized using the Bio-Rad ChemiDoc XRS+ system (Bio-Rad, Hercules, CA, USA), and relative protein expression levels were quantified using ImageJ Pro-Plus 6.0 software (Tanon, Shanghai, China).

Statistical Analysis

Data are expressed as mean ± Standard Error of the Mean (SEM). Statistical analyses were performed using GraphPad Prism version 7.0 (GraphPad Software, San Diego, CA, USA). Differences between the control and experimental groups were evaluated using a two-way Analysis of Variance (ANOVA) followed by Tukey's post hoc test. Statistical significance was denoted as follows: $^{ns}p > 0.05$, $^{*}p < 0.05$, $^{**}p < 0.01$, $^{***}p < 0.001$.

Results

Construction of Cav-1 Knockout Model and Preliminary Phenotypic Verification

The successful knockout of Cav-1 in mouse kidney tissues was confirmed by qRT-PCR and Western blot analyses, which revealed a significant reduction in Cav-1 expression ($p < 0.05$, Fig. 1A–C), verifying the effective establishment of the model. Both the WT + STZ and KO + STZ groups exhibited decreased body weight and sustained hyperglycemia throughout the 12-week modeling period, confirming the successful induction of diabetes ($p < 0.05$, Fig. 1D,E). In terms of renal functional parameters, the KO + STZ group showed significantly lower urinary albumin-creatinine ratio (UACR) levels compared with the WT + STZ group, and 24-h urinary protein excretion was also markedly reduced ($p < 0.05$, Fig. 1F,G). These findings indicate that Cav-1 deficiency partially ameliorates proteinuria induced by hyperglycemia and confers protective effects on renal function.

Effect of Cav-1 Deficiency on Renal Tissue Injury and Podocyte Alterations in Diabetic Kidney Disease

Histological analysis using H&E, PAS, and Masson's trichrome staining revealed significant pathological alterations in the WT + STZ group, including thickening of the glomerular basement membrane, interstitial fibrosis, and glycogen deposition, hallmark features of DKD. These pathological lesions were markedly attenuated in the KO + STZ group (Fig. 2A).

At the protein level, major podocyte structural markers, including Nephrin, Podocin, and Synaptopodin, were significantly downregulated in the WT + STZ group, whereas their expression levels were partially restored in the KO + STZ group (Fig. 2B–E; $p < 0.05$). These findings indicate that Cav-1 deficiency effectively mitigates podocyte structural injury.

Furthermore, the expression of endocytosis-related proteins regulated by Cav-1, including Dynamin-2, EH-domain containing protein 2 (EHD2), and Caveolae-associated protein 1 (CAVIN1), as well as signaling molecules Src family kinases (SFKs) and Ras homolog family member A (RhoA), exhibited recovery trends in the KO + STZ group compared with the WT + STZ group (Fig. 2F–K; $p < 0.05$). These findings suggest that Cav-1 may modulate podocyte injury by regulating endocytic processes and cytoskeletal signaling pathways.

Establishment of Podocyte Injury Model and Preliminary Exploration of Cav-1 Regulatory Mechanism

In HPCs, Cav-1 knockdown and Dynamin-2 overexpression cell models were established by lentiviral transduction. qRT-PCR and Western blot analyses confirmed that Cav-1 mRNA and protein levels were markedly reduced in the sh-Cav-1 group relative to the NC group ($p < 0.05$), whereas Dynamin-2 expression was significantly elevated in the OE-Dynamin-2 group ($p < 0.05$), confirming successful construction of the respective knockdown and overexpression models (Fig. 3A–F).

Upon exposure to high-glucose conditions for 48 h, both Cav-1 and Dynamin-2 protein levels were significantly upregulated (Fig. 3G–I; $p < 0.05$), suggesting that hyperglycemia induces their expression. Subsequent inhibitor interventions revealed that Cav-1 and Dynamin-2 protein expression decreased markedly under both NG and HG groups, while Dynamin-2 overexpression partially restored protein expression (Fig. 3J–L; $p < 0.05$). Collectively, these findings confirm the successful establishment of Cav-1 knockdown and Dynamin-2 overexpression models and indicate that both proteins play critical regulatory roles in high-glucose-induced podocyte injury.

Regulatory Role of Cav-1 in Podocyte Apoptosis and Endocytic Function

TUNEL staining revealed that podocyte apoptosis was significantly elevated under high-glucose conditions, whereas suppression of Cav-1 expression markedly reduced the proportion of apoptotic cells (Fig. 4A,B; $p < 0.05$). These findings suggest that Cav-1 promotes podocyte apoptosis during DKD progression and that Cav-1 deficiency confers a protective, anti-apoptotic effect. Overexpression of Dynamin-2 partially reversed the anti-apoptotic effect of Cav-1 knockdown, as indicated by a moderate increase in apoptotic cells compared with the Cav-1 knockdown group alone (Fig. 4A,B; $p < 0.05$), although apoptosis levels remained significantly lower than those in the HG + NC group.

Podocyte endocytic activity was assessed by albumin uptake assays. Endocytosis was significantly enhanced in the HG + NC group, whereas Cav-1 suppression markedly reduced intracellular albumin accumulation (Fig. 4C,D; $p < 0.05$), indicating that Cav-1 enhances receptor-mediated endocytosis in podocytes. Following Dynamin-2 overexpression in Cav-1-knockdown cells, endocytic activity significantly increased compared with the Cav-1 knockdown group ($p < 0.05$) and approached levels observed in the HG + NC group. These findings suggest that Dynamin-2 overexpression can restore endocytic capacity suppressed by Cav-1 deficiency.

Regulation of Podocyte Endocytosis-Related Protein Expression by Cav-1

Further analysis revealed that expression of classical endocytic pathway proteins, including clathrin heavy chain (CHC), Ras-related protein Rab 5 (Rab5), and Rab7, was markedly reduced in the HG + KO group (Fig. 5A–D; $p < 0.05$), indicating that Cav-1 regulates endocytic function through multiple key molecular components. Dynamin-2 overexpression significantly restored CHC, Rab5, and

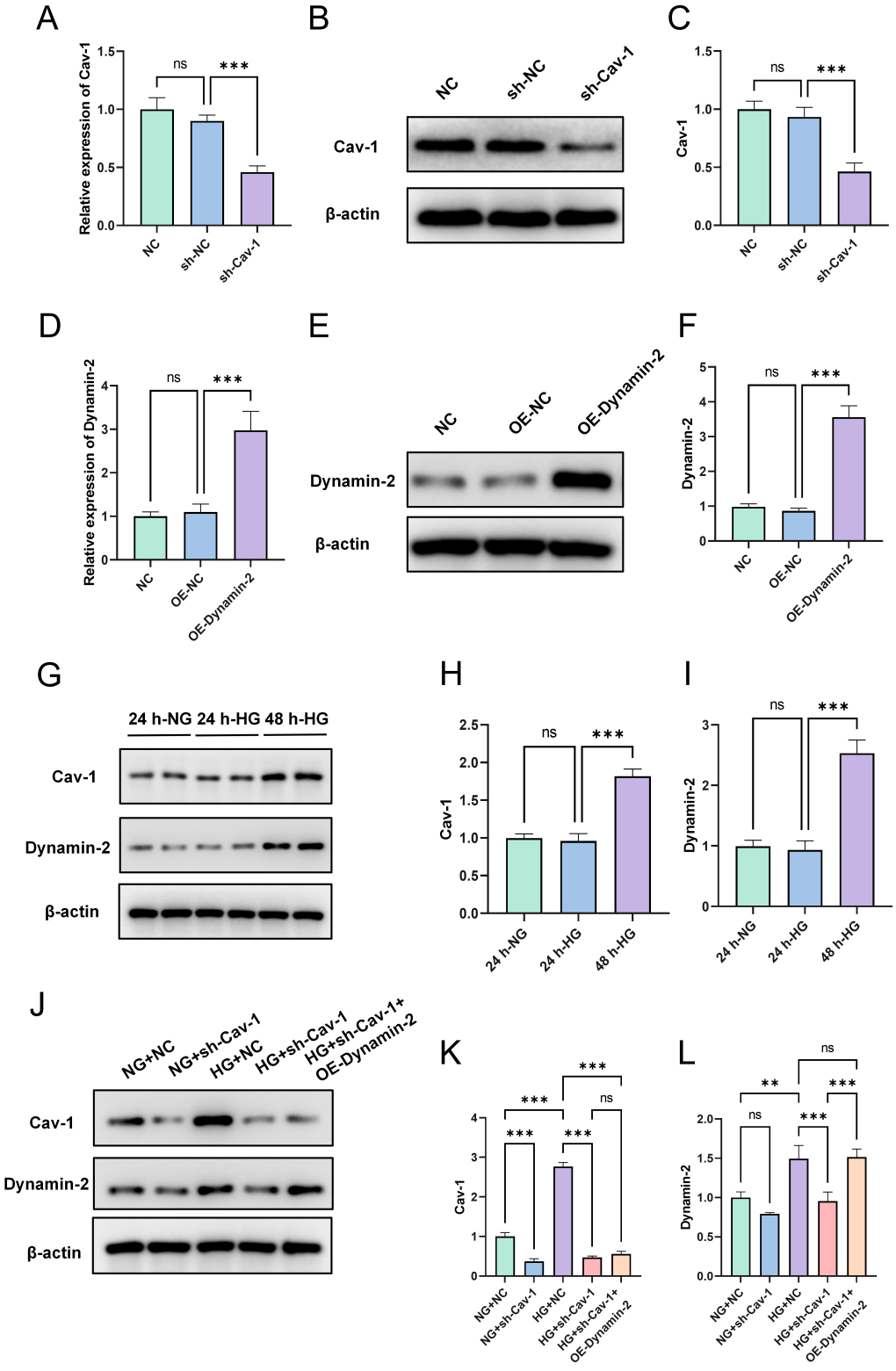

Fig. 3. Validation of Cav-1 knockdown and Dynamin-2 overexpression efficiency and their roles in high glucose-treated podocytes. (A–F) qRT-PCR and Western blot analyses confirming Cav-1 knockdown and Dynamin-2 overexpression. (G–I) Western blot analysis of Cav-1 and Dynamin-2 protein levels following high-glucose treatment. (J–L) Western blot analysis of Cav-1 and Dynamin-2 expression after inhibitor treatment and combined HG + KO + OE intervention. n = 3; ***$p < 0.001$, **$p < 0.01$, $^{ns}p > 0.05$. HG, high-glucose; NG, normal-glucose; KO, knockout; OE, overexpression.

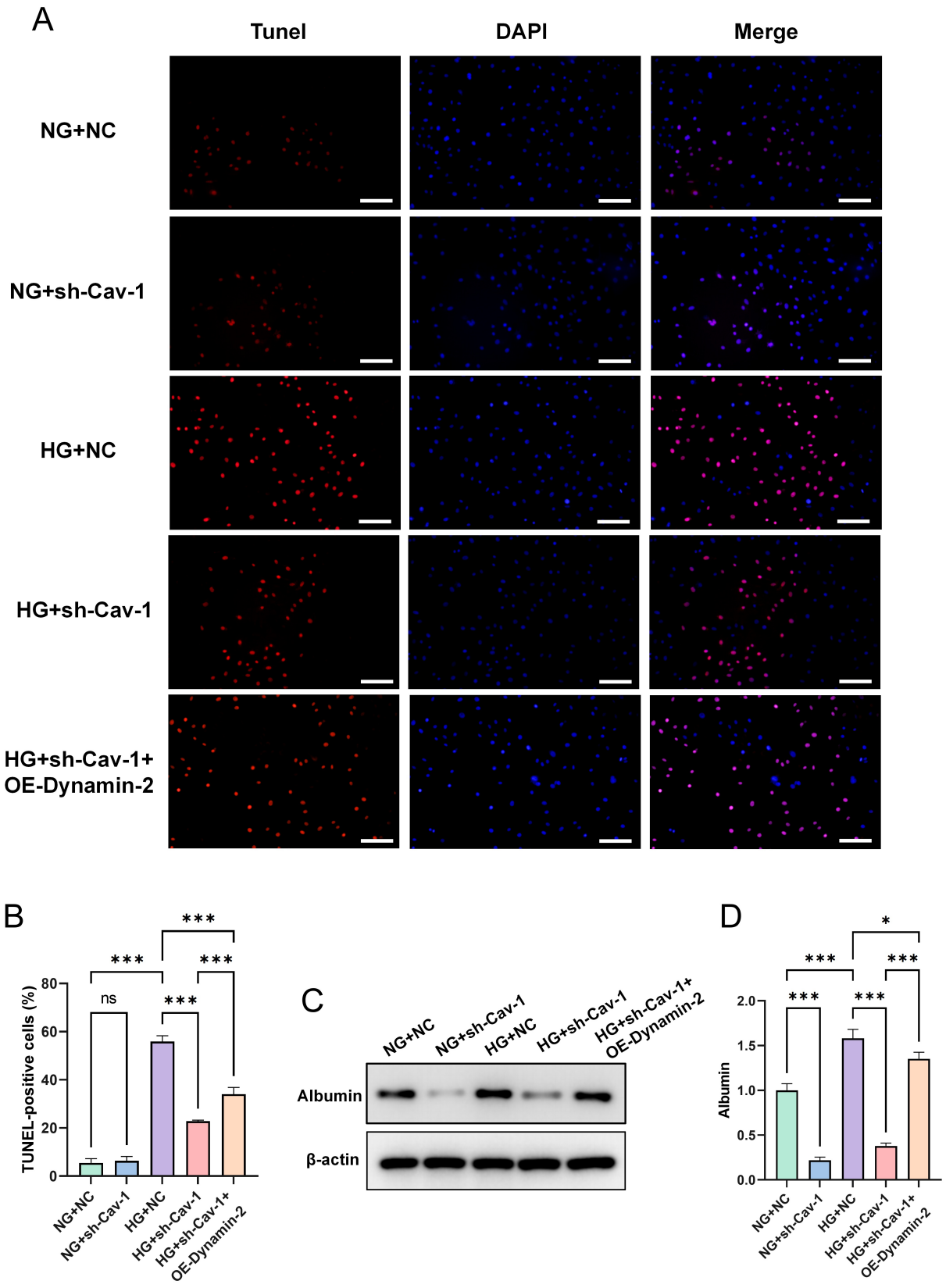

Fig. 4. Effects of Cav-1 inhibition on podocyte apoptosis and endocytic activity. (A,B) TUNEL staining showing apoptosis levels in podocytes. Scale bar: 50 µm. (C,D) Quantification of albumin endocytosis in podocytes. n = 3; ***$p < 0.001$, *$p < 0.05$, $^{ns}p > 0.05$. TUNEL, terminal deoxynucleotidyl transferase dUTP nick end labeling.

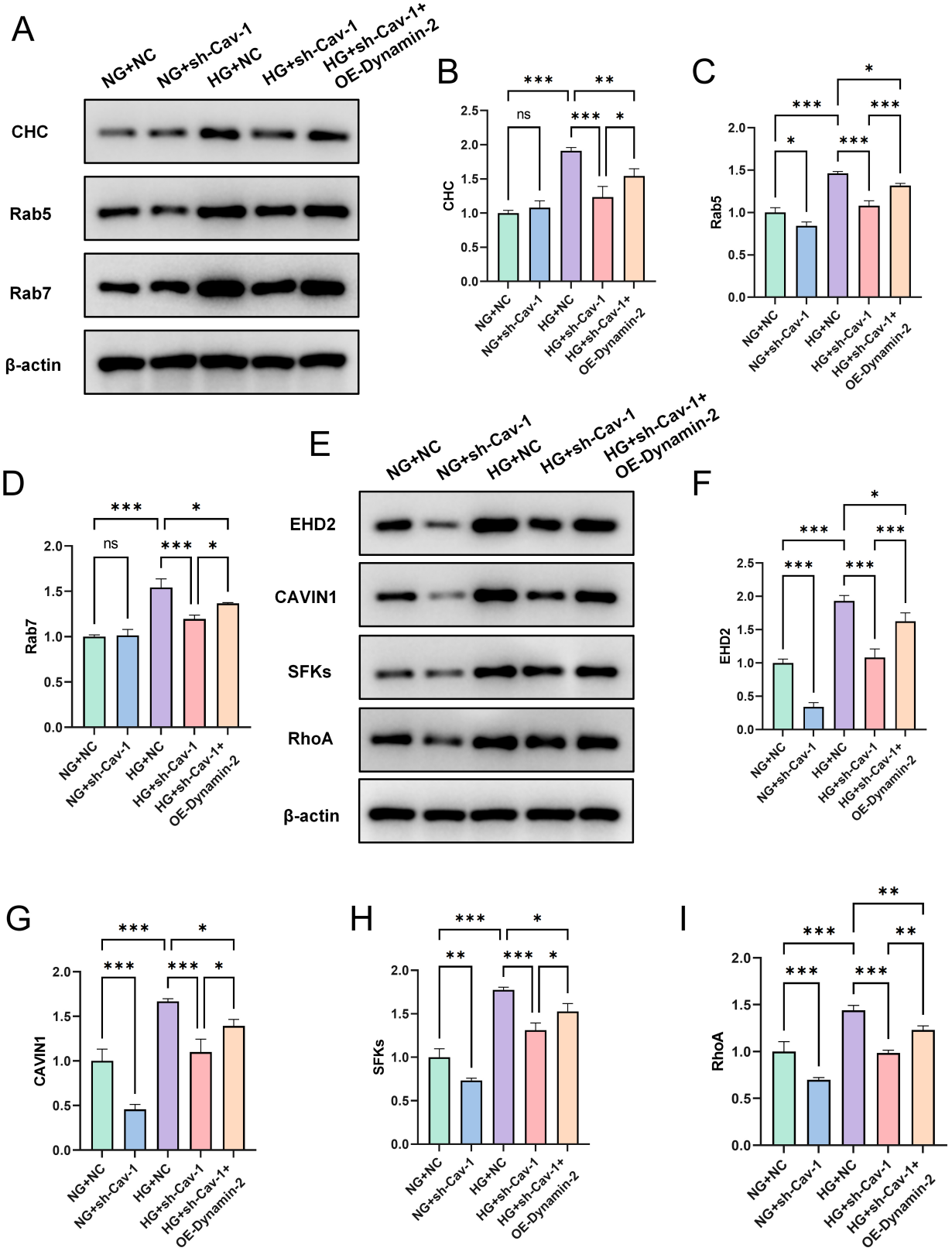

Fig. 5. Effects of Cav-1 inhibition on the expression of endocytosis-related proteins in HPC cells. (A–D) Western blot analysis of CHC, Rab5, and Rab7 protein expression levels. (E–I) Western blot analysis of EHD2, CAVIN1, SFKs, and RhoA protein expression levels. n = 3; ***$p < 0.001$, **$p < 0.01$, *$p < 0.05$, $^{ns}p > 0.05$. HPC, human podocyte; CHC, clathrin heavy chain.

Rab7 expression compared with the HG + KO group ($p < 0.05$), reaching levels comparable with those of the HG + NC group. These findings suggest partial rescue of classical endocytic pathway suppression induced by Cav-1 deficiency.

Additionally, the expression levels of EHD2, CAVIN1, SFKs, and RhoA were concomitantly downregulated in the HG + KO group (Fig. 5E–I; $p < 0.05$), suggesting that Cav-1 may modulate endocytic processes via the SFKs-RhoA signaling axis, thereby influencing podocyte function and DKD progression. Following Dynamin-2 overexpression, the expression of these molecules was significantly increased compared with the HG + KO group ($p < 0.05$), further supporting the hypothesis that Dynamin-2 exerts a compensatory effect in maintaining Cav-1-dependent endocytic signaling pathways.

Discussion

DKD is among the most common and debilitating chronic complications of diabetes and remains the leading cause of ESRD worldwide [24]. The principal pathological features of DKD include persistent proteinuria, a progressive decline in glomerular filtration rate, thickening of the glomerular basement membrane, and expansion of the mesangial matrix [25]. In recent years, increasing research attention has been directed toward glomerular podocytes, essential components of the filtration barrier, whose dysfunction is recognized as a direct driver of proteinuria and decline in renal function [8,26]. Under high-glucose conditions, podocytes are subjected to sustained oxidative stress, inflammatory stimulation, and metabolic toxicity, which readily lead to foot process effacement, cytoskeletal disorganization, mitochondrial injury, and apoptosis. These pathological alterations compromise the integrity of the glomerular filtration barrier and accelerate DKD progression [27]. Therefore, elucidating the molecular mechanisms underlying podocyte injury, especially those involving membrane structure, energy metabolism, and endocytic trafficking pathways, is of significant scientific value for understanding the fundamental pathogenesis of DKD.

Cav-1 is a principal structural protein of caveolae and a core component of membrane microdomains [28]. Cav-1 is widely expressed in epithelial cells, vascular endothelial cells, and renal podocytes, where it plays a key role in cholesterol homeostasis, lipid transport, endocytosis, and the spatial regulation of intracellular signaling molecules [14]. Previous studies have shown that Cav-1 expression is upregulated in various pathological conditions, including hyperglycemia, hyperlipidemia, and renal interstitial fibrosis, and is closely associated with tissue fibrogenesis and inflammatory responses [29,30]. However, the precise functional role of Cav-1 in podocytes during diabetic conditions remains inadequately characterized, particularly regarding its potential role in regulating podocyte endocytosis and cellular stress responses. In this study, we employed both Cav-1 knockout mouse models and high-glucose-induced HPC cell models to observe that Cav-1 expression was significantly upregulated under DKD conditions. Cav-1 deficiency markedly alleviated proteinuria, improved renal histopathological changes, and suppressed podocyte oxidative stress and apoptosis, indicating that Cav-1 may contribute to podocyte injury through stress-responsive signaling mechanisms.

Further investigation revealed that Cav-1 plays a central regulatory role in receptor-mediated endocytosis. Under high-glucose conditions, HPC cells exhibited enhanced endocytic activity, characterized by increased albumin uptake and elevated expression of key endocytosis-related proteins, including CHC, Dynamin-2, Rab5, and Rab7. However, inhibition of Cav-1 expression significantly reduced both the expression of these proteins and the overall endocytic capacity. Our findings also demonstrated that Dynamin-2 overexpression partially restored endocytic capacity and the expression of related proteins, indicating that Dynamin-2 serves a critical compensatory role in Cav-1-mediated podocyte endocytosis. This observation is consistent with recent studies reporting that Cav-1 scaffolds recruit Dynamin-2 to caveolae, thereby regulating membrane fission through its GTPase activity [31,32]. Disruption of endocytic function may impair the ability of podocytes to process extracellular nutrients and signaling molecules, consequently affecting membrane protein turnover and compromising cellular homeostasis [33]. Moreover, Cav-1 deficiency significantly suppressed the expression of Src family kinases (SFKs) and RhoA, consistent with previous findings that Cav-1 regulates podocyte cytoskeletal dynamics and apoptosis via the SFKs-RhoA signaling axis [18]. Collectively, these findings suggest that Cav-1 may act as an amplifier in high-glucose-induced podocyte injury by coordinately regulating the “endocytosis-cytoskeleton-apoptosis” pathway.

In addition, emerging evidence indicates that Cav-1 may also participate in the regulation of autophagy and mitochondrial function. For instance, Cav-1 deficiency can promote activation of the AMP-activated protein kinase (AMPK) signaling pathway, leading to the inhibition of mechanistic target of rapamycin (mTOR) activity and thereby enhancing autophagy, which alleviates cellular injury [18,34]. In this study, Cav-1 deficiency not only improved endocytic function but also significantly reduced the proportion of TUNEL-positive cells. These effects may be associated with enhanced autophagic flux or improved mitochondrial homeostasis, suggesting that future research should focus on the integrative regulatory role of Cav-1 at the convergence of multiple signaling pathways. Notably, membrane-associated proteins such as EHD2 and CAVIN1, which are functionally coupled with Cav-1, were also synchronously regulated in this study, further supporting the

central role of Cav-1 in modulating podocyte membrane structure and endocytic activity.

From a clinical translational perspective, Cav-1, as a dual-function protein involved in both structural organization and signal transduction, may serve as a potential therapeutic target for DKD. Previous studies have demonstrated that pharmacological inhibition of Cav-1 expression or its phosphorylation can effectively mitigate proteinuria and glomerular injury in animal models [18,35]. The present study further elucidates the Cav-1-mediated endocytosis-signaling regulatory mechanism and highlights the essential role of Dynamin-2, providing mechanistic evidence that supports the development of Cav-1-targeted therapeutic strategies. Moreover, recent findings suggest that SGLT2 inhibitors exert renoprotective effects, partly by modulating Cav-1 expression and associated signaling pathways. For example, empagliflozin was reported to protect glomerular endothelial cell architecture via the Vascular Endothelial Growth Factor (VEGF)-A/Cav-1/Plasmalemma Vesicle-Associated Protein-1 (PV-1) pathway, accompanied by a reduction in Cav-1 expression [36], while dapagliflozin preserves podocyte structure and function through SGLT2 inhibition in diabetic models [37]. These findings suggest the possibility that combining Cav-1-targeted inhibitors with existing clinical agents, or specifically modulating the Cav-1-Dynamin-2 axis, may represent a novel approach to delay DKD progression.

Despite the comprehensive mechanistic insights provided by this study, several limitations should be acknowledged. First, although both Cav-1 knockout mice and high-glucose-treated human podocytes were utilized, the *in vivo* findings were derived from global knockout models rather than podocyte-specific Cav-1 deletion, which may introduce confounding effects from other renal cell types. Second, while this work focused on Dynamin-2 as a principal mediator of Cav-1-regulated endocytosis, additional interacting proteins or signaling pathways may also contribute to podocyte injury in DKD. Third, the translational relevance of these findings warrants further validation using patient-derived samples and additional preclinical models. Future research should address these limitations to better elucidate the complex regulatory networks underlying podocyte injury and the progression of diabetic kidney disease.

Conclusion

In summary, this study systematically elucidates the pathogenic role of Cav-1 in podocyte injury during diabetic kidney disease from multiple perspectives, including alterations in the expression of structural protein, regulation of signaling pathways, and changes in cellular function. As a key effector of Cav-1-mediated endocytosis, Dynamin-2 can partially compensate for the endocytic impairments resulting from Cav-1 deficiency, suggesting a functional interdependence between these two proteins in vesicular trafficking. Targeting Cav-1 and its associated SFKs-RhoA signaling axis, along with Dynamin-2-mediated endocytic and autophagic pathways, may offer novel therapeutic strategies and precise intervention approaches for DKD. Future investigations should further elucidate the molecular interactions among Cav-1, Dynamin-2, and other podocyte regulatory pathways, such as autophagy, ferroptosis, and mitochondrial dynamics, and validate their therapeutic potential using cell-type-specific animal models and clinical specimens to facilitate the translation of mechanistic insights into clinical applications.

Availability of Data and Materials

The datasets used and/or analyzed during the current study are available from the corresponding authors upon reasonable request.

Author Contributions

XW designed the research study and drafted the manuscript. YX, CL, and XF performed the experiments and collected the data. KC and YZ provided technical support and advice on data analysis. All authors contributed to the critical revision of the manuscript for important intellectual content. All authors read and approved the final manuscript. All authors have met the four ICMJE authorship criteria and agreed to be accountable for all aspects of the work.

Ethics Approval and Consent to Participate

All animal experiments were approved by the Laboratory Animal Management and Ethics Committee of Zhejiang Chinese Medical University (Approval No. 20250217-07) and were conducted in accordance with institutional guidelines and the international standards for animal care and use to ensure ethical treatment of animals.

Acknowledgment

Not applicable.

Funding

This research received no external funding.

Conflict of Interest

The authors declare no conflict of interest.

References

[1] Yu X, Li Y, Zhang Y, Yin K, Chen X, Zhu X. Leonurine Ameliorates Diabetic Nephropathy through GPX4-Mediated Ferroptosis of Endothelial Cells. Frontiers in Bioscience (Landmark Edition). 2024; 29: 270. https://doi.org/10.31083/j.fbl2907270.

[2] Mohandes S, Doke T, Hu H, Mukhi D, Dhillon P, Susztak K. Molecular pathways that drive diabetic kidney disease. The Journal of Clinical Investigation. 2023; 133: e165654. https://doi.org/10.1172/JCI165654.

[3] Zhang R, Wang Q, Li Y, Li Q, Zhou X, Chen X, *et al*. A new perspective on proteinuria and drug therapy for diabetic kidney disease. Frontiers in Pharmacology. 2024; 15: 1349022. https://doi.org/10.3389/fphar.2024.1349022.

[4] Ding X, Zhang D, Ren Q, Hu Y, Wang J, Hao J, *et al*. Identification of a Non-Invasive Urinary Exosomal Biomarker for Diabetic Nephropathy Using Data-Independent Acquisition Proteomics. International Journal of Molecular Sciences. 2023; 24: 13560. https://doi.org/10.3390/ijms241713560.

[5] Naaman SC, Bakris GL. Diabetic Nephropathy: Update on Pillars of Therapy Slowing Progression. Diabetes Care. 2023; 46: 1574–1586. https://doi.org/10.2337/dci23-0030.

[6] Tan SK, Pinzon-Cortes JA, Cooper ME. Novel pharmacological interventions for diabetic kidney disease. Current Opinion in Nephrology and Hypertension. 2024; 33: 13–25. https://doi.org/10.1097/MNH.0000000000000935.

[7] Wang N, Zhang C. Recent Advances in the Management of Diabetic Kidney Disease: Slowing Progression. International Journal of Molecular Sciences. 2024; 25: 3086. https://doi.org/10.3390/ijms25063086.

[8] Liu S, Yuan Y, Xue Y, Xing C, Zhang B. Podocyte Injury in Diabetic Kidney Disease: A Focus on Mitochondrial Dysfunction. Frontiers in Cell and Developmental Biology. 2022; 10: 832887. https://doi.org/10.3389/fcell.2022.832887.

[9] Yang C, Zhang Z, Liu J, Chen P, Li J, Shu H, *et al*. Research progress on multiple cell death pathways of podocytes in diabetic kidney disease. Molecular Medicine (Cambridge, Mass.). 2023; 29: 135. https://doi.org/10.1186/s10020-023-00732-4.

[10] Barutta F, Bellini S, Gruden G. Mechanisms of podocyte injury and implications for diabetic nephropathy. Clinical Science (London, England: 1979). 2022; 136: 493–520. https://doi.org/10.1042/CS20210625.

[11] Tian X, Bunda P, Ishibe S. Podocyte Endocytosis in Regulating the Glomerular Filtration Barrier. Frontiers in Medicine. 2022; 9: 801837. https://doi.org/10.3389/fmed.2022.801837.

[12] Simón L, Campos A, Leyton L, Quest AFG. Caveolin-1 function at the plasma membrane and in intracellular compartments in cancer. Cancer Metastasis Reviews. 2020; 39: 435–453. https://doi.org/10.1007/s10555-020-09890-x.

[13] Dalton CM, Schlegel C, Hunter CJ. Caveolin-1: A Review of Intracellular Functions, Tissue-Specific Roles, and Epithelial Tight Junction Regulation. Biology. 2023; 12: 1402. https://doi.org/10.3390/biology12111402.

[14] Chidlow JH, Jr, Sessa WC. Caveolae, caveolins, and cavins: complex control of cellular signalling and inflammation. Cardiovascular Research. 2010; 86: 219–225. https://doi.org/10.1093/cvr/cvq075.

[15] Miao F, Lei Y, Guo Y, Ma Y, Zhang Y, Jia B. Increased caveolin 1 by human antigen R exacerbates Porphyromonas gingivalis-induced atherosclerosis by modulating oxidative stress and inflammatory responses. CytoJournal. 2024; 21: 42. https://doi.org/10.25259/Cytojournal_76_2024.

[16] Liu J, Yao J, Zhao Y, Su J, Ye J, Wang Y. Angiopoietin2-mediated caveolin1 phosphorylation regulating transcytosis of renal tubular epithelial cell contributes to the occurrence of albuminuria under high glucose exposure. Journal of Translational Medicine. 2022; 20: 185. https://doi.org/10.1186/s12967-022-03388-6.

[17] Sun LN, Liu XC, Chen XJ, Guan GJ, Liu G. Curcumin attenuates high glucose-induced podocyte apoptosis by regulating functional connections between caveolin-1 phosphorylation and ROS. Acta Pharmacologica Sinica. 2016; 37: 645–655. https://doi.org/10.1038/aps.2015.159.

[18] Luo S, Yang M, Zhao H, Han Y, Jiang N, Yang J, *et al*. Caveolin-1 Regulates Cellular Metabolism: A Potential Therapeutic Target in Kidney Disease. Frontiers in Pharmacology. 2021; 12: 768100. https://doi.org/10.3389/fphar.2021.768100.

[19] Van Krieken R, Krepinsky JC. Caveolin-1 in the Pathogenesis of Diabetic Nephropathy: Potential Therapeutic Target? Current Diabetes Reports. 2017; 17: 19. https://doi.org/10.1007/s11892-017-0844-9.

[20] Hamasaki E, Wakita N, Yasuoka H, Nagaoka H, Morita M, Takashima E, *et al*. The Lipid-Binding Defective Dynamin 2 Mutant in Charcot-Marie-Tooth Disease Impairs Proper Actin Bundling and Actin Organization in Glomerular Podocytes. Frontiers in Cell and Developmental Biology. 2022; 10: 884509. https://doi.org/10.3389/fcell.2022.884509.

[21] Mukherjee K, Gu C, Collins A, Mettlen M, Samelko B, Altintas MM, *et al*. Simultaneous stabilization of actin cytoskeleton in multiple nephron-specific cells protects the kidney from diverse injury. Nature Communications. 2022; 13: 2422. https://doi.org/10.1038/s41467-022-30101-4.

[22] Bayonés L, Guerra-Fernández MJ, Figueroa-Cares C, Gallo LI, Alfonso-Bueno S, Caspe O, *et al*. Dynamin-2 mutations linked to neonatal-onset centronuclear myopathy impair exocytosis and endocytosis in adrenal chromaffin cells. Journal of Neurochemistry. 2024; 168: 3268–3283. https://doi.org/10.1111/jnc.16194.

[23] Shao M, Yue Y, Sun GY, You QH, Wang N, Zhang D. Caveolin-1 regulates Rac1 activation and rat pulmonary microvascular endothelial hyperpermeability induced by TNF-α. PloS One. 2013; 8: e55213. https://doi.org/10.1371/journal.pone.0055213.

[24] American Diabetes Association. 11. Microvascular Complications and Foot Care: *Standards of Medical Care in Diabetes-2021*. Diabetes Care. 2021; 44: S151–S167. https://doi.org/10.2337/dc21-S011.

[25] Tervaert TWC, Mooyaart AL, Amann K, Cohen AH, Cook HT, Drachenberg CB, *et al*. Pathologic classification of diabetic nephropathy. Journal of the American Society of Nephrology: JASN. 2010; 21: 556–563. https://doi.org/10.1681/ASN.2010010010.

[26] Reidy K, Kang HM, Hostetter T, Susztak K. Molecular mechanisms of diabetic kidney disease. The Journal of Clinical Investigation. 2014; 124: 2333–2340. https://doi.org/10.1172/JCI72271.

[27] Forbes JM, Thorburn DR. Mitochondrial dysfunction in diabetic kidney disease. Nature Reviews. Nephrology. 2018; 14: 291–312. https://doi.org/10.1038/nrneph.2018.9.

[28] Parton RG. Caveolae: Structure, Function, and Relationship to Disease. Annual Review of Cell and Developmental Biology. 2018; 34: 111–136. https://doi.org/10.1146/annurev-cellbio-100617-062737.

[29] Haddad D, Al Madhoun A, Nizam R, Al-Mulla F. Role of Caveolin-1 in Diabetes and Its Complications. Oxidative Medicine and Cellular Longevity. 2020; 2020: 9761539. https://doi.org/10.1155/2020/9761539.

[30] Zhang D, Gava AL, Van Krieken R, Mehta N, Li R, Gao B, *et al*. The caveolin-1 regulated protein follistatin protects against diabetic kidney disease. Kidney International. 2019; 96: 1134–1149. https://doi.org/10.1016/j.kint.2019.05.032.

[31] Matthaeus C, Taraska JW. Energy and Dynamics of Caveolae Trafficking. Frontiers in Cell and Developmental Biology. 2021; 8: 614472. https://doi.org/10.3389/fcell.2020.614472.

[32] Yao Q, Chen J, Cao H, Orth JD, McCaffery JM, Stan RV, *et al*. Caveolin-1 interacts directly with dynamin-2. Journal of Molecular Biology. 2005; 348: 491–501. https://doi.org/10.1016/j.jmb.2005.02.003.

[33] Swiatecka-Urban A. Endocytic Trafficking at the Mature Podocyte Slit Diaphragm. Frontiers in Pediatrics. 2017; 5: 32.

https://doi.org/10.3389/fped.2017.00032.

[34] Wang Y, Liu Z, Shu S, Cai J, Tang C, Dong Z. AMPK/mTOR Signaling in Autophagy Regulation During Cisplatin-Induced Acute Kidney Injury. Frontiers in Physiology. 2020; 11: 619730. https://doi.org/10.3389/fphys.2020.619730.

[35] Zhao M, Cao Y, Ma L. New insights in the treatment of DKD: recent advances and future prospects. BMC Nephrology. 2025; 26: 72. https://doi.org/10.1186/s12882-025-03953-3.

[36] Locatelli M, Zoja C, Conti S, Cerullo D, Corna D, Rottoli D, *et al*. Empagliflozin protects glomerular endothelial cell architecture in experimental diabetes through the VEGF-A/caveolin-1/PV-1 signaling pathway. The Journal of Pathology. 2022; 256: 468–479. https://doi.org/10.1002/path.5862.

[37] Cassis P, Locatelli M, Cerullo D, Corna D, Buelli S, Zanchi C, *et al*. SGLT2 inhibitor dapagliflozin limits podocyte damage in proteinuric nondiabetic nephropathy. JCI Insight. 2018; 3: e98720. https://doi.org/10.1172/jci.insight.98720.